

The inverse Compton catastrophe and high brightness temperature radio sources

O. Tsang and J. G. Kirk

Max-Planck-Institut-für Kernphysik, Saupfercheckweg 1, D-69117 Heidelberg, Germany

Received ... / Accepted ...

ABSTRACT

Context. The inverse Compton catastrophe is the dramatic rise in the luminosity of inverse-Compton scattered photons predicted to occur when the synchrotron brightness temperature exceeds a threshold value, usually estimated to be 10^{12} K. However, this effect appears to be in contradiction with observation because: (i) the threshold is substantially exceeded by several intra-day variable radio sources, but the inverse Compton emission is not observed, (ii) powerful, extra-galactic radio sources of known angular size do not appear to congregate close to the predicted maximum brightness temperature.

Aims. We re-examine the parameter space available to synchrotron sources using a non-standard electron distribution, in order to see whether the revised threshold temperature is consistent with the data.

Methods. We apply the theory of synchrotron radiation to a population of monoenergetic electrons. The electron distribution and the population of each generation of scattered photons are computed using spatially averaged equations. The results are formulated in terms of the electron Lorentz factors that characterise sources at the threshold temperature and sources in which the particle and magnetic field energy density are in equipartition.

Results. We confirm our previous finding that intrinsic brightness temperatures $T_B \sim 10^{14}$ K can occur without catastrophic cooling. We show that substantially higher temperatures cannot be achieved either in transitory solutions or in solutions that balance losses with a powerful acceleration mechanism. Depending on the observing frequency, we find strong cooling can set in at a range of threshold temperatures and the imposition of the additional constraint of equipartition between particle and magnetic field energy is not warranted by the data.

Conclusions. Postulating a monoenergetic electron distribution, which approximates one that is truncated below a certain Lorentz factor (γ_{\min}), alleviates several theoretical difficulties associated with the inverse Compton catastrophe, including anomalously high brightness temperatures and the apparent lack of clustering of powerful sources at 10^{12} K.

Key words. galaxies: active – galaxies: high redshift – galaxies: jets

1. Introduction

When interpreting the synchrotron spectrum of powerful extra-galactic radio sources, it is usual to assume that the underlying electron distribution has a power-law form $dN/d\gamma \propto \gamma^{-q}$. For a homogeneous source, the spectrum peaks at the point $\nu = \nu_{\text{abs}}$, where the optical depth to synchrotron self-absorption is of the order of unity, and above this frequency the intensity falls off as $I_\nu \propto \nu^{-(q-1)/2}$. Because more electrons become effective at absorbing the radiation as the frequency decreases, the optically thick part of the spectrum is not of the Rayleigh-Jeans type, but has instead $I_\nu \propto \nu^{5/2}$, independent of the power-law index of the underlying distribution, (provided $q > 1/3$). Correspondingly, the brightness temperature peaks at $\nu \approx \nu_{\text{abs}}$, falling off as $\nu^{1/2}$ to

lower and as $\nu^{-(q+3)/2}$ to higher frequencies. In this case, Kellermann & Pauliny-Toth (1969) found that the ratio of the luminosity L_{IC} carried away by inverse Compton scattered photons to that of synchrotron photons L_s is

$$\frac{L_{\text{IC}}}{L_s} = \left(\frac{T_B}{T_{\text{thresh}}} \right)^5 \left[1 + \left(\frac{T_B}{T_{\text{thresh}}} \right)^5 \right] \quad (1)$$

where T_B is the intrinsic brightness temperature at the peak of the radio emission and $T_{\text{thresh}} \approx 10^{12}$ K, depending somewhat on the parameter q and the maximum frequency at which synchrotron radiation is emitted, corresponding to an assumed cut-off in the power-law electron spectrum (Readhead 1994).

The rapid rise in total luminosity implied by Eq. (1) when T_B exceeds T_{thresh} is called the “inverse Compton catastrophe”. The implied energy requirement of a 1 Jy source at $z = 1$ is $\sim 10^{43}$ ergs s^{-1} at $T_B = 10^{12}$ K, and a prohibitive $\sim 10^{53}$ ergs s^{-1} at $T_B = 10^{13}$ K at

1GHz. A source of 1GHz photons with magnetic field $\approx 1\mu\text{G}$, boosts a radio photon into the X-ray band in a single inverse Compton scattering. At $T_{\text{B}} = 10^{12}\text{K}$ this would imply a nanoJansky X-ray flux, not untypical of strong extragalactic sources. However, at $T_{\text{B}} = 10^{13}\text{K}$ Eq. (1) predicts an X-ray flux at the milliJansky level, in contradiction with observation (Fossati et al. 1998; Sambruna et al. 2000; Tavecchio et al. 2002; Padovani et al. 2004; Guainazzi et al. 2006).

Despite this, several sources that display intra-day variability (IDV) in their radio emission have an implied brightness temperature that exceeds 10^{12}K by several orders of magnitude, if the observed variability is intrinsic (e.g., Kraus et al. 2003). Even if the variability is caused by scintillation, the implied brightness temperature can still greatly exceed 10^{12}K for some sources (Wagner & Witzel 1995). Currently, the most extreme example is the source PKS 0405-385. This source displays diffractive scintillation (Macquart & de Bruyn 2005), which places an upper limit on its angular size that corresponds to a brightness temperature of $2 \times 10^{14}\text{K}$. These sources are generally assumed to be *beamed*, i.e., to be in relativistic motion towards the observer (e.g., Rees 1966; Jones & Burbidge 1973; Singal & Gopal-Krishna 1985). In this case the intrinsic temperature is lower than that deduced for a stationary source by a factor of \mathcal{D}^3 (for intrinsic variability) or \mathcal{D} (for scintillating sources). (Here the Doppler factor $\mathcal{D} = \sqrt{1 - \beta^2}/(1 - \beta \cos \theta)$ with βc the source velocity and θ the angle between this velocity and the line of sight.) Nevertheless, the observed brightness temperatures are too high to be accounted for by Doppler factors similar to those estimated from observations of superluminal motion (Cohen et al. 2003).

A second problem arises with powerful sources whose angular extent can be measured directly. In an analysis of high brightness temperature radio sources in which Doppler beaming is thought to be absent, Readhead (1994) measured a brightness distribution that cuts off at 10^{11}K ; one order of magnitude lower than the inverse Compton limit. This appears consistent with observations of a sample of 48 sources showing superluminal motion (Cohen et al. 2003), in which it was found that the intrinsic brightness temperature cluster around $2 \times 10^{10}\text{K}$. Readhead (1994) argued that an apparent maximum brightness temperature significantly lower than 10^{12}K could not be caused by catastrophic Compton cooling. Instead, he suggested that sources are driven towards equipartition between their magnetic and particle energy contents. Assuming, in addition, that observations are taken at the peak of the synchrotron spectrum, and that the electron distribution is a power-law, he showed that the expected distribution of brightness temperatures was consistent with that observed.

In this paper, we re-examine these two problems assuming that the source contains a monoenergetic electron distribution instead of the conventional power-law. Although this assumption appears at first sight highly re-

strictive, the form of the synchrotron emissivity means that under some circumstances such a distribution provides a good approximation to several more commonly encountered cases, including that of a conventional power-law distribution that is truncated to lower energy at a Lorentz factor γ_{min} . Such distributions have been proposed in connection with radio sources for a variety of reasons: the absence of low energy electrons can account for the lack of Faraday depolarisation in parsec-scale emission regions (Wardle 1977; Jones & Odell 1977) and has recently been discussed in connection with statistical trends in the observed distribution of superluminal velocities as a function of observing frequency and redshift (Gopal-Krishna et al. 2004). Also, Blundell et al. (2006) recently examined the radio and x-ray emission from the lobe regions of a giant radio galaxies 6C 0905+3955, and deduced a low energy cutoff of the relativistic particles in the hotspots of $\gamma_{\text{min}} \sim 10^4$.

In Sect. 2 we use standard theory to discuss the general properties of the synchrotron spectra emitted by a homogeneous source. A set of spatially averaged equations describing the evolution of the electron Lorentz factor and both the synchrotron and the associated inverse Compton scattered emission is presented in Sect. 3. Having identified in these equations the threshold for the inverse Compton catastrophe, we discuss the parameter space available to stationary solutions in Sect. 4. Here we confirm the results reported in Kirk & Tsang (2006), indicating that temperatures considerably in excess of 10^{12}K are permitted. We also show that in the case of resolved sources, the onset of catastrophic cooling occurs over a wide range of temperatures, consistent with the observed temperature range. Finally, we address in Sect. 5 the suggestions by Slysh (1992) that extremely high brightness temperatures can be achieved in nonstationary sources either by injecting electrons at high energy, or by balancing their cooling against a powerful acceleration mechanism. A summary of our conclusions is presented in Sect. 6.

2. Synchrotron spectra

We consider a homogeneous source region characterised by a single spatial scale R , that contains monoenergetic electrons and possibly positrons of Lorentz factor γ and number density n_e immersed in a magnetic field B . Expressions for the synchrotron emissivity and absorption coefficients can be found in many excellent texts (e.g., Rybicki & Lightman (1979, Chapter 6), and Longair (1992, chapter 18)) and are summarised in our notation in Appendix A.

For any given source there exists a frequency ν_{abs} below which absorption is important. Since B and γ also define a characteristic synchrotron frequency ν_s (see Eq. A.3), the sources we consider can be divided into two categories: those with *weak absorption* in which $\nu_{\text{abs}} < \nu_s$ and those with *strong absorption* $\nu_{\text{abs}} > \nu_s$. Note that this division is independent of the observing frequency, since it relates only to intrinsic source properties. The synchrotron

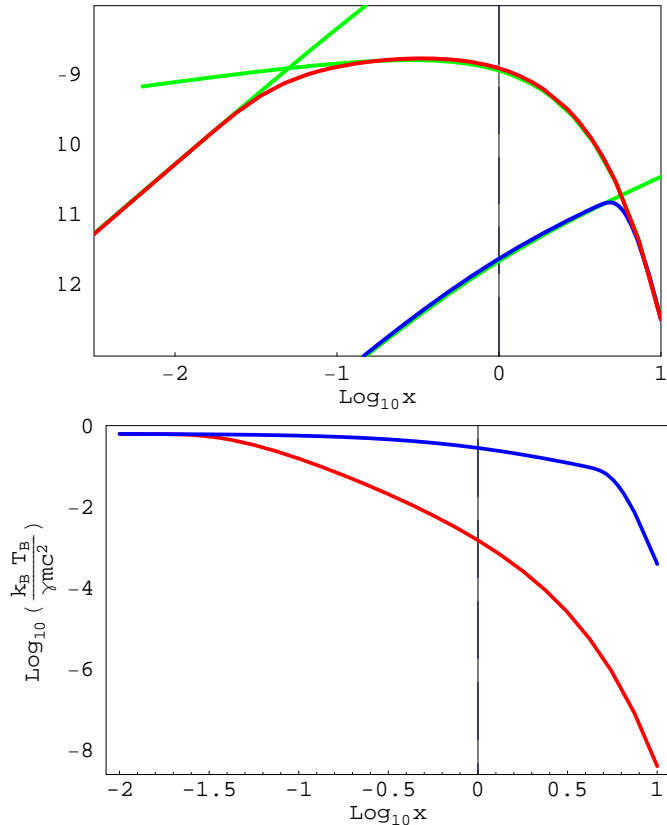


Fig. 1. The synchrotron spectra (upper panel) and brightness temperatures (lower panel) of sources with monoenergetic electrons in the case of strong (blue) and weak (red) absorption. The green curves show the optically thick ($I_\nu = S_\nu$, see Appendix A) and optically thin ($I_\nu = \tau_s S_\nu$) approximation. In the upper panel, I_ν is in arbitrary units, and in the lower, the brightness temperature is normalised to the energy of the electron. The abscissa x is the ratio of the frequency to the characteristic synchrotron frequency of the electrons ν_s . The blue (red) curves correspond to a source which has an optical depth of unity to synchrotron self-absorption at $x \approx 5$ ($x \approx 0.05$). For ease of display, the upper panel compares sources with equal flux at high frequency, whereas the lower compares sources with equal flux at low frequency.

spectra that emerge in these two cases are quite different, and are illustrated in Fig. 1. A feature they have in common is that the low energy spectrum has the Rayleigh-Jeans form $I_\nu \propto \nu^2$, where I_ν is the specific intensity at frequency ν . This property contrasts with the $\nu^{5/2}$ dependence of I_ν at low frequencies of a source containing a power-law distribution of electrons. The reason is that a power-law distribution contains cold (low energy) electrons that contribute to the absorption at low frequencies.

The brightness temperature, $T_B = c^2 I_\nu / (2\nu^2 k_B)$, where k_B is Boltzmann’s constant, is a function of frequency and is also illustrated in Fig. 1. At low frequency, it attains its maximum value roughly in “equilibrium” with the electrons: $T_{B,\max} = 3\gamma m c^2 / 4k_B$, then decreases monotonically to higher frequencies. In the case of weak

absorption, $T_{B,\max} \propto \nu^{-5/3}$ for $\nu_{\text{abs}} < \nu < \nu_s$, and then cuts off exponentially as $\nu^{-3/2} \exp(-\nu/\nu_s)$ once ν_s is exceeded. In strongly absorbed sources, the brightness temperature remains almost constant until the frequency exceeds ν_s upon which it falls off as ν^{-1} until the source becomes optically thin, after which the exponential cut-off $T \propto \nu^{-3/2} \exp(-\nu/\nu_s)$ takes over.

Although four parameters (γ , n_e , B and R) are needed to define a source model, the division between strong and weak absorption is simple. It occurs at a critical Lorentz factor γ_c given by (see Eq. A.11)

$$\gamma_c = 324 \times \left(\frac{n_e}{1 \text{ cm}^{-3}} \right)^{1/5} \left(\frac{R}{1 \text{ kpc}} \right)^{1/5} \left(\frac{B}{1 \text{ mG}} \right)^{-1/5} \quad (2)$$

or, equivalently,

$$\gamma_c = 4451 \times \tau_T^{1/5} \left(\frac{B}{1 \text{ mG}} \right)^{-1/5} \quad (3)$$

where $\tau_T = n_e R \sigma_T$ is the Thomson optical depth of the source. Strong absorption occurs for low Lorentz factors $\hat{\gamma} = \gamma/\gamma_c < 1$ and weak absorption for high Lorentz factors $\hat{\gamma} > 1$. If the Lorentz factor γ is held constant, the strong absorption regime may be reached from the weak by increasing τ_T at constant B , or by *decreasing* B at constant τ_T .

In his model of high-brightness temperature sources, Slysh (1992) considered the strong absorption case. The most important property of the assumed distribution in this case is the lack of high energy electrons: the addition of a population of cold electrons, which would correspond to a power-law distribution truncated to higher Lorentz factors, would reduce the brightness temperature of the source at $x < 1$ (in Fig. 1) but would not significantly influence this quantity, for $x > 1$.

On the other hand, Crusius-Waetzel (1991) and Protheroe (2003) considered weak absorption, where the key property of the model distribution is the absence of low energy electrons. In this case, the monoenergetic model is a good approximation to a power-law distribution truncated to lower electron energies at $\gamma = \gamma_{\min}$. The addition of a high-energy power-law tail affects the spectrum at $x > 1$, but does not change the maximum brightness temperature achieved at $x \lesssim 1$. Furthermore, the truncation need not be sharp: provided the opacity at low frequencies is dominated by the contribution of electrons with $\gamma \approx \gamma_{\min}$, the monoenergetic approximation is good. This is the case if, for $\gamma < \gamma_{\min}$, the spectrum is sufficiently hard: $dN/d\gamma \propto \gamma^{-q}$ with $q \leq 1/3$. In particular, the low energy tail of a relativistic Maxwellian distribution ($q = -2$) falls into this category.

In contrast to the pure power-law distribution, where the self-absorption turnover is strongly peaked, the emission of a weakly absorbed source — shown in red in the upper panel of Fig. 1 — is flat over nearly two decades in frequency. It therefore provides a natural explanation of compact flat-spectrum sources, eliminating the need to appeal to a “cosmic conspiracy” behind the superposition of

peaked spectra from different parts of an inhomogeneous source (Marscher 1980).

For the treatment of inverse Compton scattering, it is necessary to evaluate the energy density U_s in synchrotron photons in a given source. To do this, I_ν must be integrated over angles and over frequency. The result depends on the geometry and optical depth as well as the position within the source. An average value can be estimated by introducing a geometry dependent factor, ζ , defined according to:

$$U_s \approx \frac{4\pi\zeta}{c} \int_0^\infty d\nu \langle I_\nu \rangle \quad (4)$$

where $\langle I_\nu \rangle$ is conveniently taken to be the specific intensity along a ray path that is within the source for a distance R and is perpendicular to the local magnetic field. Protheroe (2002) has evaluated ζ for several interesting special cases. For a roughly spherical source, it is of the order of unity. Below, we show that the choice $\zeta = 2/3$ is consistent with our spatially averaged treatment of the kinetic equations. The dominant contribution to the integral over the spectrum arises from photons of frequency close to ν_s in the case of weak absorption, and close to ν_{abs} in the case of strong absorption. Using this approximation, for weak absorption ($\hat{\gamma} > 1$):

$$U_s \approx 4.1 \times 10^{-6} \gamma^2 \zeta \left(\frac{B^2}{8\pi} \right) \left(\frac{n_e}{1 \text{ cm}^{-3}} \right) \left(\frac{R}{1 \text{ kpc}} \right) \quad (5)$$

or, equivalently,

$$U_s \approx 2\gamma^2 \tau_T \zeta \left(\frac{B^2}{8\pi} \right) \quad (6)$$

and for strong absorption ($\hat{\gamma} < 1$):

$$U_s \approx 8.9 \times 10^{-18} \gamma_c^7 \zeta \left(\frac{B^2}{8\pi} \right) \left(\frac{B}{1 \text{ mG}} \right) (\ln \hat{\gamma})^2 \quad (7)$$

An approximation that is accurate for all values of the optical depth is given in Eq. (A.24).

3. Spatially averaged equations

An approximate, spatially averaged set of equations governing the energy balance of particles and synchrotron radiation in a source can be found following the approach of Lightman & Zdziarski (1987) and Mastichiadis & Kirk (1995). In terms of the time-dependent synchrotron radiation energy density $U_0(t)$ one can write:

$$\frac{dU_0}{dt} + c \langle \alpha_\nu \rangle U_0 + \frac{c}{R} U_0 = \langle j_\nu \rangle \quad (8)$$

The second and third terms on the left-hand side of this equation represent the rate of energy loss by the radiation field due to synchrotron self-absorption and escape through the source boundaries; the right-hand side is the power put into radiation by the particles. The angle brackets indicate a frequency and angle average, but, within this spatially-averaged treatment, an exact calculation of the frequency average is unnecessary; it suffices to replace the

absorption coefficient by its value where the energy density of the synchrotron spectrum peaks i.e., at $\nu = \nu_s$ in the case of weak absorption and $\nu = \nu_{\text{abs}}$ in the case of strong absorption. In terms of the optical depth to synchrotron absorption at this point, $\tau_p \leq 1$, the equation becomes:

$$\frac{dU_0}{dt} + \frac{c}{R} (1 + \tau_p) U_0 = \langle j_\nu \rangle \quad (9)$$

The right-hand side of this expression can now be found by demanding it gives the correct steady solution at both large and small optical depth. The resulting equation is:

$$\frac{dU_0}{dt} + \frac{c}{R} (1 + \tau_p) [U_0(t) - U_s(\gamma)] = 0 \quad (10)$$

where U_s is the steady-state synchrotron radiation energy density, evaluated according to Eq. (4), with an appropriate value of the parameter ζ .

The corresponding equation for the particles that takes into account synchrotron absorption and emission as well as an acceleration term takes the form

$$n_e m c^2 \frac{d\gamma}{dt} = \frac{c}{R} \tau_p U_0 - \frac{c}{R} (1 + \tau_p) U_s + a e B c n_e \quad (11)$$

The first term on the right-hand side of Eq. (11) is the power taken from the radiation field by self-absorption and the second term is that returned to it — both of these appear in Eq. (10). The third term describes the energy input by particle acceleration. The particular scaling used follows that of Slysh (1992), and models a generic first-order Fermi process. For a independent of γ , the acceleration rate is proportional to the gyro frequency, and for $a = 1$ it equals this value. The acceleration timescale equals the crossing time of the source when $a = \gamma m c^2 / (e B R)$.

Multiple inverse Compton scatterings can be accounted for as follows: First we label the photons present in the source according to how many scattering events they have suffered after production by the synchrotron process. The energy density of these photons is denoted by U_i . Thus, $i = 0$ corresponds to photons emitted by the synchrotron process which have not undergone a scattering, and the corresponding energy density is governed by Eq. (10). Assuming the source is optically thin to Thomson (or Compton) scattering, the dominant loss mechanism for the energy density of photons belonging to a given generation $i \geq 1$ is escape from the source, rather than conversion to the $i + 1$ 'th generation. In this case, we can write for the time-dependence of U_i :

$$\frac{dU_i}{dt} + \frac{c}{R} U_i = Q_i \quad (12)$$

where Q_i is the rate per unit volume at which energy is transferred into photons of the i 'th generation by inverse Compton scattering, for $i \geq 1$, or by synchrotron radiation for $i = 0$.

If the inverse scattering process proceeds in the Thomson regime a simple expression can be found for Q_i . However, as i increases, $h\nu_i$ also increases, eventually becoming comparable to the electron energy when viewed in

its rest frame. When this happens, Klein-Nishina modifications to the Thomson cross section become important, reducing the value Q_i . We take approximate account of this effect by limiting the number of scatterings to N_{\max} , and using the Thomson approximation to evaluate Q_i for $i \leq N_{\max}$. In this case, the average energy of a scattered photon of the i 'th generation is $\nu_i = 4\gamma^2\nu_{i-1}/3$ and the rate of such scatterings in unit volume of the source is $n_e\sigma_T c U_{i-1}/(h\nu_{i-1})$. Therefore

$$Q_i = \begin{cases} \xi c U_{i-1}/R & \text{for } 1 \leq i \leq N_{\max} \\ 0 & \text{for } i > N_{\max} \end{cases} \quad (13)$$

where the parameter ξ is defined as

$$\begin{aligned} \xi &= \frac{4}{3} n_e \sigma_T R \gamma^2 \\ &= \frac{4\gamma^2 \tau_T}{3} \end{aligned} \quad (14)$$

The appropriate value of N_{\max} is chosen by requiring the average energy of the N_{\max} generation of photons viewed in the electron rest frame $\gamma(4\gamma^2/3)^{N_{\max}} h\nu_0$ to be less than the electron energy:

$$N_{\max} = \text{floor} \left[\frac{\ln(mc^2/h\nu_0)}{2 \ln \gamma} + \frac{1}{2} \right] \quad (15)$$

For synchrotron radiation, Eq. (10) implies

$$Q_0 = \frac{c\tau_p}{R} (U_s - U_0) + \frac{c}{R} U_s \quad (16)$$

In the stationary case, $U_0 = U_s$, Eqs. (13) and (16) give $Q_1/Q_0 = \xi$. However, assuming scattering in the Thomson regime, the ratio of the energy lost by synchrotron radiation to that by inverse Compton scattering in the steady state equals the ratio of the energy density of the magnetic field to that of the target photons $Q_0/Q_i = B^2/(8\pi U_{i-1})$, which, for $i = 0$, implies $U_s = \xi(B^2/8\pi)$. Comparison with Eq. (6) then confirms that the spatially averaged kinetic equations are consistent with the choice $\zeta = 2/3$ for the geometry dependent factor. Finally, the electron equation (11) acquires the additional loss terms from inverse Compton scattering:

$$n_e mc^2 \frac{d\gamma}{dt} = - \sum_{i=0}^{N_{\max}} Q_i + a e B c n_e \quad (17)$$

The set of equations (12) and (17) can be rewritten by introducing the total energy density of scattered radiation:

$$U_T = \sum_{i=1}^{N_{\max}} U_i \quad (18)$$

Then, using dimensionless variables according to $\hat{U} = U(8\pi/B^2)$, $\hat{t} = tc/R$ and $\hat{Q}_i = 8\pi c Q_i/(RB^2)$ one finds

$$\frac{d\hat{U}_T}{d\hat{t}} + [1 - \xi] \hat{U}_T = \xi (\hat{U}_0 - \hat{U}_{N_{\max}}) \quad (19)$$

If $U_{N_{\max}}$ remains always negligibly small, then all significant scatterings occur in the Thomson regime, and the set of equations (12) (for $i = 0$), (17), and (19) can be conveniently formulated in terms of three characteristic values of the Lorentz factor:

$$\frac{d\hat{U}_T}{d\hat{t}} = - \left[1 - (\gamma/\gamma_{\text{cat}})^2 \right] \hat{U}_T + (\gamma/\gamma_{\text{cat}})^2 \hat{U}_0 \quad (20)$$

$$\frac{d\hat{U}_0}{d\hat{t}} = -\hat{U}_0 + \hat{Q}_0 \quad (21)$$

$$\frac{d\gamma}{d\hat{t}} = -\gamma_{\text{eq}} \left[\hat{Q}_0 + (\gamma/\gamma_{\text{cat}})^2 \hat{U}_T \right] + \gamma_{\text{tr}} a \quad (22)$$

where γ_{eq} is chosen so that there is equipartition between particle and magnetic energy densities for $\gamma = \gamma_{\text{eq}}$:

$$\gamma_{\text{eq}} = B^2/(8\pi n_e mc^2) \quad (23)$$

γ_{cat} is given by setting $\xi = 1$

$$\gamma_{\text{cat}} = \sqrt{\frac{3}{4\tau_T}} \quad (24)$$

and γ_{tr} corresponds to the maximum Lorentz factor of a particle that can be confined in the source, i.e., whose gyro-radius is less than R :

$$\gamma_{\text{tr}} = eBR/(mc^2) \quad (25)$$

The significance of γ_{cat} can be seen from the steady state solution of Eqs. (20) and (21): $U_T = U_s/(\gamma_{\text{cat}}^2/\gamma^2 - 1)$. For values of γ that approach γ_{cat} from below, the energy density in the radiation field, and, hence, the luminosity diverge. Thus, under the assumption that all scatterings take place in the Thomson limit, no stationary solutions can be found for

$$\gamma \geq \gamma_{\text{cat}} \quad (26)$$

This phenomenon is the nonrelativistic or ‘‘Thomson’’ manifestation of the *Compton catastrophe* described in the Introduction. In the weak absorption limit, $\hat{U}_s = \gamma^2/\gamma_{\text{cat}}^2$, confirming the well-known result that the Compton catastrophe sets in when the energy density in synchrotron photons exceeds the magnetic energy density. However, this result does not apply to the case of strong absorption, where we find $\hat{U}_s \sim \gamma_{\text{cat}}^5/\gamma_c^5 \ll 1$. In this regime, the synchrotron radiation energy density can be much smaller than the energy density in the magnetic field at the point where catastrophic cooling sets in. Physically, the scattered photons feed on each other to produce the catastrophe in this regime, and do not require a substantial synchrotron photon density. In a realistic model, the divergence of the luminosity is prevented by Klein-Nishina effects, that effectively truncate the series in Eq. (18). For example, if $T_{B,\max} = 10^{12}$ K, at an observing frequency of 1 GHz, so that $\gamma \approx 200$, then, from Eq. (15), the number of terms contributing to the sum is $N_{\max} = 2$.

4. Stationary solutions

4.1. Intra-day variable sources

For comparison with observations of intra-day variable sources, it is convenient to formulate the expression for the specific intensity given in Eq. (A.15) in terms of quantities accessible to observation. Expressing the result in terms of the observed (at $z = 0$) brightness temperature, we find, in the case of weak absorption, and at low frequency ($\nu \ll \nu_s$)

$$T_B = 1.2 \times 10^{14} \left(\frac{\mathcal{D}_{10}^6 \xi}{(1+z)^6} \right)^{1/5} \left(\frac{1 - e^{-\tau_s}}{\tau_s^{1/5}} \right) \nu_{\max,14}^{2/15} \nu_{\text{GHz}}^{-1/3} \text{ K} \quad (27)$$

(Kirk & Tsang 2006) where $\mathcal{D} = 10\mathcal{D}_{10}$ is the Doppler boosting factor, z is the redshift of the host galaxy, τ_s is the optical depth of the source at the observing frequency $\nu = \nu_{\text{GHz}}$ GHz, and the characteristic synchrotron frequency of the electrons is $\nu_s = \nu_{\max,14} \times 10^{14}$ Hz.

According to Eq. (27), brightness temperatures of $T_B \approx 10^{13}$ K, such as observed in the sources PKS 1519 –273 and PKS 0405 –385 (Macquart et al. 2000; Rickett et al. 2002) can be understood within a simplified homogeneous synchrotron model in which $\xi \lesssim 1$, implying a relatively modest inverse Compton luminosity, i.e., no catastrophe. Even the extremely compact source J 1819 +3845, which has $T_B \gtrsim 2 \times 10^{14}$ K can be accommodated in a catastrophe-free model provided the Doppler factor is greater than about 15. In each case, a hard spectrum is predicted, extending to $\nu_{\max,14} \times 10^{14}$ Hz. Although the dependence of the brightness temperature on this parameter is quite weak, simultaneous observations in the radio to IR and optical (Ostorero et al. 2006) have the potential to rule out this explanation on a source by source basis.

4.2. Resolved sources

In a seminal paper, Readhead (1994) discussed the distribution in brightness temperature of a sample of powerful sources whose angular size could either be measured directly, or constrained by interplanetary scintillation. In discussing these objects several simplifications must be made, even within the context of a homogeneous synchrotron model.

Firstly, in the two low frequency samples (81.5 MHz and 430 MHz) considered by Readhead (1994), the emission is thought to be almost isotropic. Doppler boosting is then unimportant and can be neglected. Secondly, these sources are not very compact; their extension on the sky is typically between 0.1 and 1 arcsec. Therefore, for our discussion we fix the linear extent R of the source to 1 kpc, corresponding to an angular size of approximately 0.2 arcsec at redshift $z = 1$. This leaves three parameters needed to specify the source model: the magnetic field strength B , the electron density n_e and the Lorentz factor γ of the electrons. In order to clarify the physics of a source, we transform from the parameter set (B, n_e, γ)

to the characteristic Lorentz factors γ_{eq} and γ_{cat} defined in Eqs. (23) and (24). Our basic parameter set is therefore $(\gamma_{\text{eq}}, \gamma_{\text{cat}}, \gamma)$. Finally, in order to display on a two-dimensional figure source properties such as brightness temperature and spectral slope at a particular frequency, we consider a slice through this three dimensional parameter space, selecting parameters such that the particle and magnetic energy densities are in equipartition: $\gamma = \gamma_{\text{eq}}$.

The properties of source models on this slice are shown in the $\gamma_{\text{eq}} - \gamma_{\text{cat}}$ plane in Fig. 2. This plane can immediately be divided into regions of strong and weak absorption, as defined in Eq. (2). The boundary, drawn as a thick dashed line, represents the locus of the points at which $\gamma_c = \gamma_{\text{eq}}$. Weakly absorbed sources lie towards higher γ_{eq} and γ_{cat} (i.e., the upper-right side) and strongly absorbed sources towards lower γ_{eq} and γ_{cat} (i.e., the lower-left side). We also show (in blue) contours of the magnetic field strength.

The remaining source properties depend upon the choice of observing frequency. In Fig. 2 we take this to be 81.5 MHz, corresponding to the low frequency sample discussed by Readhead (1994). In order to determine the spectral slope of a given source, we plot as a yellow line the locus of points where the observing frequency coincides with the frequency at which the optical depth to absorption is unity, ν_{abs} . Sources that lie above this line (on the side of larger γ_{cat}) are optically thin at the chosen observing frequency. In addition, the red line in Fig. 2 gives the locus of points where the observing frequency equals the characteristic frequency of synchrotron radiation ν_c . By definition, the intersection point of these lines lies also on the boundary between weak and strong absorption (the thick dashed line). The observing frequency lies below ν_c on the lower-right side of the red line. The colour shading gives the intrinsic brightness temperature at the chosen observing frequency.

The two lines (yellow and red) divide the $\gamma_{\text{eq}} - \gamma_{\text{cat}}$ -plane in Fig. 2 into four regions with differing spectral properties: in region A, sources have a Rayleigh-Jeans spectrum $I_\nu \propto \nu^2$, in region B, the spectrum is that of low frequency, optically thin synchrotron radiation $I_\nu \propto \nu^{1/3}$, in region C, it is close to $I_\nu \propto \nu$ (see Slysh 1992) and in region D it falls off exponentially $I_\nu \propto \nu^{-1/2} \exp(-\nu/\nu_c)$. Consequently, flat spectrum sources reside in region B, preferentially close to the yellow line and in region C, preferentially close to the red line.

Sources that are in equipartition and lie below the threshold of the Compton catastrophe are to be found in the upper left half of Fig. 2, above the dotted line on which $\gamma_{\text{eq}} = \gamma_{\text{cat}}$. The maximum brightness temperature accessible to these sources occurs close to $\gamma_{\text{eq}} = \gamma_{\text{cat}} = 10^3$, and is approximately $10^{12.6}$ K, in rough agreement with the results of Kellermann & Pauliny-Toth (1969), who, however, did not assume their sources to be in equipartition. The brightest sources are weakly absorbed, (they lie to the right of the thick dashed line) and have a magnetic field strength of a few milliGauss. Their optical depth to synchrotron self-absorption lies close to unity at the observation frequency (they lie close to the yellow line).

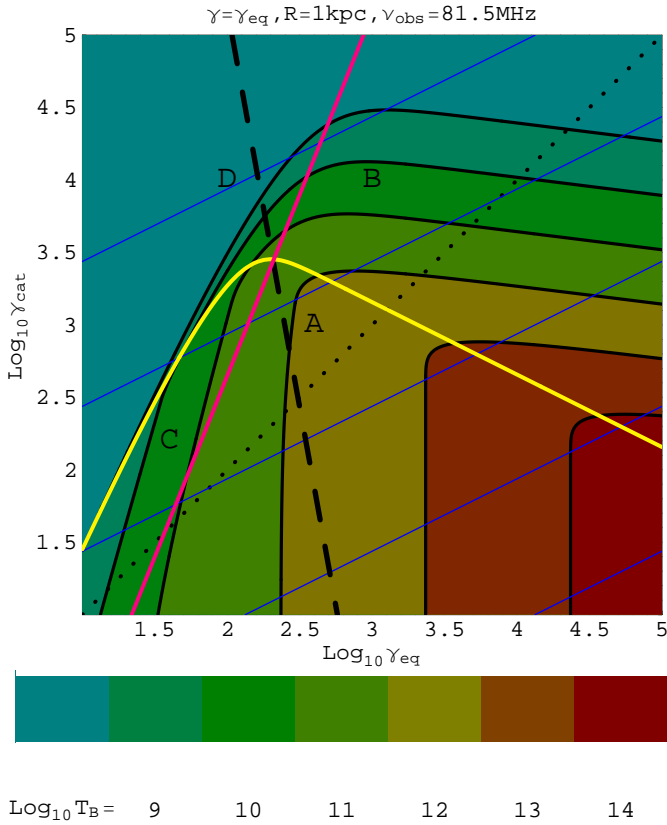


Fig. 2. The brightness temperature as a function of γ_{eq} and γ_{cat} assuming equipartition between the magnetic and particle energy densities and a source size 1 kpc. Black contour lines indicate $\log_{10}(T/\text{Kelvin}) = 9, 10, 11, 12, 13$ and 14 . The red line is the locus of points at which the characteristic synchrotron frequency of the emitting particles is 81.5 MHz, the yellow line shows where the source has an optical depth of unity at this frequency. The dashed line divides regions of strong absorption (to the left) from those of weak absorption (to the right). The diagonal $\gamma_{\text{eq}} = \gamma_{\text{cat}}$ is shown as a dotted line. Contour lines of the magnetic field strength are shown in blue, ranging from $\log_{10}(B/\text{Gauss}) = -4$ to 0 (in the bottom right-hand corner).

Singal & Gopal-Krishna (1985) first discussed the effects of the additional assumption of equipartition on bright sources and used it to estimate Doppler factors for rapidly variable sources. Later, Readhead (1994) introduced the concept of an “equipartition brightness temperature” to explain the observation that the temperature distribution of resolved sources appears to peak significantly below 10^{12} K. However, the crucial additional assumptions in his treatment is that the source flux is measured at the “synchrotron peak”, and that the electron distribution is a power-law in energy. This implies that the opacity at a given frequency (e.g., at the synchrotron peak) is dominated by those electrons with a corresponding characteristic frequency. In our model, in which the electron distribution is approximated as monoenergetic, these assumptions are roughly equivalent to demanding

that the source lies on the red line in Fig. 2 if it is weakly absorbed (i.e., on the boundary of regions B and D), and on the yellow line if it is strongly absorbed (i.e., on the boundary of regions C and D). This leads to a maximum brightness temperature of a few times 10^{10} K, as found by Readhead (1994). Furthermore, as noted by Readhead (1994), such sources lie far from the threshold temperature, achieved along the dotted line in Fig. 2.

Replacing the assumption that the source flux is measured at the synchrotron peak, by the requirement that its spectrum be flat, i.e., that it lie in region B of Fig. 2, one sees that a wide range of brightness temperatures is available for sources in equipartition, extending up to the threshold temperature found by Kellermann & Pauliny-Toth (1969). Thus, the observed temperature distribution is not explained by the assumption of equipartition.

5. Time dependence and acceleration

In order to explain the occurrence of brightness temperatures above 10^{12} K, Slysh (1992) formulated a model involving a monoenergetic electron distribution in a strongly absorbed source, in the sense that $\gamma < \gamma_c$, where γ_c is defined in Eqs. (2) and (3). He considered two scenarios, (i) a time-dependent one in which electrons were injected at arbitrarily high Lorentz factors and allowed to cool and (ii) one in which a strong continuous re-acceleration of the electrons led to a high brightness temperature equilibrium.

In each case, the assumption that the source is strongly absorbed leads to extreme values of the parameters. For example, in the first scenario in which high energy particles are injected into the source, Slysh (1992) finds that a brightness temperature of $T_{\text{B}} > 5 \times 10^{15}$ K can be sustained over 1 day at an observing frequency of 1 GHz. This is clearly in conflict with our analysis. The electron Lorentz factor required to achieve this temperature is $\gamma > 10^5$. However, the condition that the source is strongly absorbed, which is used in this model to estimate the cooling rate, combined with the condition $\nu_s \approx 1$ GHz required for a flat spectrum, leads to an extremely large Thomson optical depth, $\tau \approx 130$, as well as an implausibly low magnetic field $B \approx 2 \times 10^{-11}$ G. The parameter ξ that determines the inverse Compton luminosity is approximately 10^{12} , which implies an extremely large compactness of the inverse Compton radiation from the source. The resulting copious pair production invalidates the analysis and, ultimately, reduces the brightness temperature achievable in the radio range. The same criticism applies also to the second scenario described by Slysh (1992) in which acceleration balances inverse Compton losses to provide a brightness temperature of 10^{14} K at 1 GHz.

In the absence of Klein-Nishina effects on the scattering cross section, we find the time dependence of the particle and photon energies can be described by the three ordinary differential equations (20), (21) and (22). Inspection of these shows that if the threshold temperature is ex-

ceeded ($\gamma > \gamma_{\text{cat}}$), the inverse Compton luminosity grows in a timescale of roughly the light-crossing time of the source. Thus, the threshold can only be substantially exceeded if the acceleration process in Eq. (22) operates on a shorter timescale. However, these equations employ a spatial average over the emission region. Although a rapid acceleration rate might be achieved locally in small regions of the source, once an average is taken, no timescale in the system can be shorter than the light-crossing time of the region over which the accelerated particles are distributed. In this case, the threshold temperature cannot be significantly exceeded.

At first sight, Klein-Nishina effects offer a possible escape from this conclusion. If even the first order scattering is suppressed, which requires extremely large Lorentz factors for the electrons ($\gamma > 10^{10}$ is needed for Klein-Nishina effects when scattering 10 GHz photons), the strong reduction in the rate of cooling by inverse Compton scattering suggests that higher brightness temperatures T_B might be possible.

This is, however, not the case, because the rate of production of electron-positron pairs by photon-photon interactions becomes important. The strength of this effect, which is not included in our model equations, can be measured in terms of the ‘‘compactness parameter’’ ℓ (see, for example Mastichiadis & Kirk 1995), defined as

$$\ell = \frac{\sigma_T R U_{N_{\text{max}}}}{h\nu_{N_{\text{max}}}} \quad (28)$$

where $U_{N_{\text{max}}}$ is defined in Eq. (12), N_{max} in Eq. (15), and $\nu_{N_{\text{max}}}$ is taken to be $(4\gamma^2/3)^{N_{\text{max}}}\nu_0$. When $\ell > 1$, one expects the pair-production rate to be roughly equal to the light-crossing time of the source. This leads to a sharp rise in the Thomson optical depth, invalidating the assumption of scatter-free escape of synchrotron photons that is implicit in our model. The associated confinement of these photons reduces the brightness temperature.

We illustrate this in Fig. 3, where we compare two models with the same linear size R (and observing frequency), but different electron densities n_e and different values of B , chosen as follows: For any given set of parameters, R , B and n_e , and observing frequency ν_{obs} , the optical depth to synchrotron absorption τ_s , as defined in Eq. (A.12), has a single maximum as a function of γ , located close to the point where ν_{obs} equals the characteristic synchrotron frequency. If the source is optically thick to absorption at this point, then $\gamma < \gamma_c$, as described in Sect. 2, and the brightness temperature is roughly $3\gamma mc^2/4k_B$. If, on the other hand, the source is optically thin at this point, then $\gamma > \gamma_c$, but the brightness temperature, given approximately by $\tau_s \times 3\gamma mc^2/4k_B$, decreases to higher γ , as can be seen from Eq. (A.12). Thus, assuming inverse Compton scattering does not intervene, the maximum brightness temperature is observed at a frequency such that $\tau_s \approx 1$, when $\gamma = \gamma_c$, which implies $x \approx 1$. These conditions are imposed on the parameters of the models presented in Fig. 3. In addition to the source size, chosen to be $R = 0.01$ pc and the observing frequency,

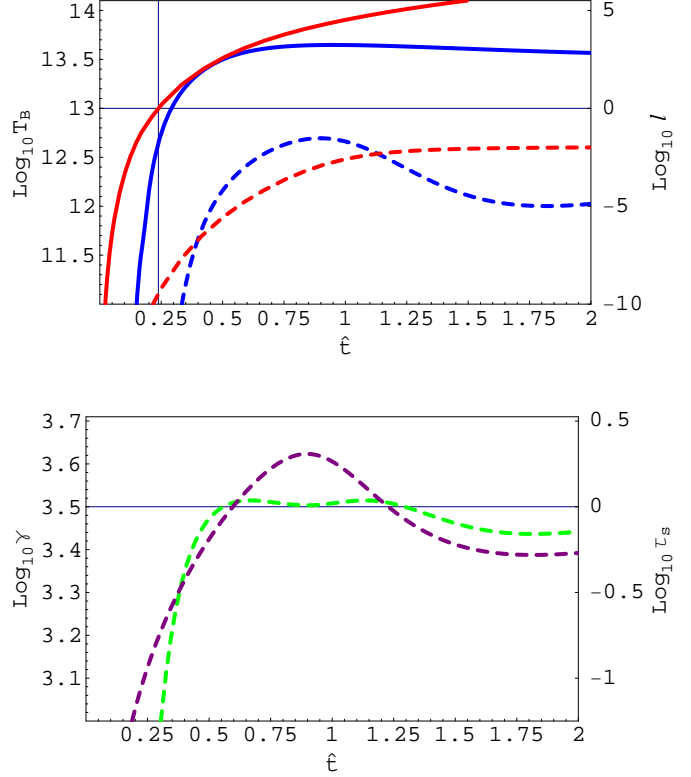


Fig. 3. *Upper panel:* The brightness temperature T_B (blue), and the compactness ℓ (red) as functions of time, for two stationary, local sources ($\mathcal{D} = 1$, $z = 0$) with linear size $R = 0.01$ pc, observed at 1 GHz. The Thomson optical depth is $\tau_T = 0.01$ (dashed lines) and $\tau_T = 1$ (solid lines) and the remaining parameters are chosen such that the optical depth to synchrotron self-absorption $\tau_s \approx 1$ at $\gamma = \gamma_c$ (see Eqs. (2) and (3)). A horizontal line is drawn to indicate $\ell = 1$. *Lower panel:* The electron Lorentz factor (purple dashed) and the optical depth to synchrotron self-absorption τ_s (green dashed) for the case $\tau_T = 0.01$. A horizontal line indicates $\tau_s = 1$.

set to 1 GHz, this leaves one free parameter, which we choose to be the optical depth to Thomson scattering τ_T .

The upper panel in Fig. 3 shows the time-dependence of the brightness temperature found by solving Eqs. (12) and (17) numerically for sources with $\tau_T = 0.01$ (dashed blue line) and $\tau_T = 1$ (solid blue line), without allowance for Doppler boosting ($\mathcal{D} = 1$). These sources have $\gamma_c = 10^{3.6}$ and $\gamma_c = 10^{4.3}$, respectively and, in the absence of inverse Compton cooling, they could potentially achieve brightness temperatures of $T_B \approx 10^{13.2}$ K and $T_B \approx 10^{13.9}$ K. In order to do so, rapid acceleration is required, since for these source parameters, inverse Compton cooling leads to a time-asymptotic value of the Lorentz factor that is somewhat lower than γ_c for slow acceleration. The exact value of the asymptotic solution depends on the strength of the acceleration. For acceleration on the light-crossing timescale, it corresponds to

$a \approx \gamma/\gamma_{\text{tr}}$ [see Eq. (22)]. In Fig. 3 we choose $a = 1.5\gamma/\gamma_{\text{tr}}$, which leads to an overshoot that slightly exceeds γ_c .

For $\tau_T = 0.01$, the compactness, shown as a function of time by the red dashed line, remains well below unity, so that the effects of pair production can be neglected. However, this is not the case for $\tau_T = 1$. Here, the compactness (solid red line) rises rapidly, reaching unity at $\hat{t} \approx 0.25$, where $T_B \approx 3.5 \times 10^{12}$ K, well below its potential maximum. Thus, the attempt to gain higher brightness temperature by increasing τ_T , and, hence, γ_c , leads to a breakdown in the model assumptions due to pair production.

The lower panel of Fig. 3 shows the electron Lorentz factor and the optical depth to synchrotron self-absorption τ_s as functions of time for the case $\tau_T = 0.01$. The Lorentz factor overshoots both its time-asymptotic value and γ_c . Correspondingly, the optical depth, (shown as the green dashed line) which initially rises with γ , reaching unity at $\gamma = \gamma_c$ goes through a maximum very shortly afterwards. However, the overshoot is not sufficient to push τ_s back below unity, and the maximum brightness temperature, which coincides with the maximum Lorentz factor, remains at $T_B = 5 \times 10^{12}$ K, somewhat below the value of $T_B \approx 10^{13.2}$ K, estimated for large optical depth.

6. Conclusions

The well-known upper limit on the brightness temperature of a synchrotron source $T_B \lesssim 10^{12}$ K imposed by the inverse Compton catastrophe, has been reassessed, assuming a monoenergetic electron distribution.

In weakly absorbed sources (see Eq. (2)), this distribution mimics the situation in which the conventional power-law is truncated to lower energies at a Lorentz factor γ_{min} . Using the standard theory of synchrotron emission and self-absorption, we find that, for such sources, the brightness temperature at a frequency of a few GHz can reach approximately 10^{14} K, the precise limit being given in Eq. (27). Physically, this increased limit reflects the absence of cool electrons in monoenergetic distributions and in those that are truncated or hard below a certain Lorentz factor. As a consequence, intra-day variable sources can in principle be understood without recourse to other mechanisms such as unusually large Doppler factors (Rees 1967), coherent emission (e.g., Begelman et al. 2005) or proton synchrotron radiation (Kardashev 2000).

The possibility of exceeding the new limit in a time-dependent solution by balancing losses against a strong acceleration term has been investigated using a set of spatially averaged equations. Provided the acceleration process remains causal i.e., the acceleration time averaged over the source remains longer than the light-crossing time, we find a modest overshoot is possible, but the maximum temperature is still restricted by Eq. (27). In strongly absorbed sources, such as those considered by Slyph (1992), high brightness temperatures cannot be attained in a self-consistent model of the kind we discuss. The underlying reason is that extremely compact sources

would be required, in which copious pair-production must be taken into account.

We have examined in detail the parameter space available to homogeneous synchrotron sources of fixed size. In the case of flat spectrum sources, we find that the imposition of the condition of equipartition between the particle and magnetic field energy densities does not result in a lower limit on the brightness temperature than that given by the inverse Compton catastrophe. Suggestions to the contrary (Readhead 1994) are based on the more restrictive twin assumptions that the power-law electron distribution is not truncated within the relevant range, and that the temperature is measured at the point where the optical depth of the source is approximately unity. Consequently, the observed temperature distribution does not support the equipartition hypothesis. We also find that flat spectrum sources close to equipartition can approach the threshold temperature of the inverse Compton catastrophe, in contrast with the finding based on the more restrictive assumptions in Readhead (1994).

A corollary of the theory presented here is that for very bright sources, which are necessarily weakly absorbed, a high degree of intrinsic circular polarisation is predicted (Kirk & Tsang 2006). In addition, the theory can be tested by comparison of the predicted synchrotron spectrum with simultaneous observations of high brightness temperature sources in the radio to infra-red range and comparison of the predicted inverse Compton emission with measurements at MeV to GeV energies.

Appendix A: Synchrotron formulae

We consider a region of homogeneous magnetic field B , linear dimension R , (and volume R^3) containing monoenergetic electrons/positron of number density n_e and Lorentz factor γ . The volume emissivity for synchrotron radiation, summed over polarisations, is:

$$j_\nu = \frac{\sqrt{3}}{4\pi} n_e \alpha_f \hbar \Omega_L \sin \theta F(x) \quad (\text{A.1})$$

$$x = \nu/\nu_c \quad (\text{A.2})$$

$$\nu_c(\gamma, \theta) = \frac{3\Omega_L \sin \theta \gamma^2}{4\pi} = \nu_0 \gamma^2 \quad [\nu_0 = 3\Omega_L \sin \theta / (4\pi)] \quad (\text{A.3})$$

$$F(x) = x \int_x^\infty dt K_{5/3}(t) \quad (\text{A.4})$$

where $\alpha_f = e^2/\hbar c$ is the fine-structure constant, $\Omega_L = eB/mc$ the Larmor frequency and θ the angle between the magnetic field and the direction of the emitted radiation. For small and large x the limiting forms are

$$F(x) \approx \frac{4\pi}{\sqrt{3}\Gamma(1/3)} \left(\frac{x}{2}\right)^{1/3} \quad \text{for } x \ll 1 \quad (\text{A.5})$$

$$F(x) \rightarrow \sqrt{\frac{\pi x}{2}} e^{-x} \quad \text{for } x \rightarrow \infty \quad (\text{A.6})$$

The absorption coefficient for unpolarised radiation is

$$\alpha_\nu = \frac{1}{2\sqrt{3}} \frac{n_e \sigma_T}{\alpha_f b \sin \theta} \frac{K_{5/3}(x)}{\gamma^5} \quad (\text{A.7})$$

where $b = \hbar\Omega_L/mc^2$ is the magnetic field in units of the critical field $B_c = 4.414 \times 10^{13}$ G and σ_T is the Thomson cross-section. The limiting forms are:

$$K_{5/3}(x) \approx \frac{2^{2/3}\Gamma(5/3)}{x^{5/3}} \quad \text{for } x \ll 1 \quad (\text{A.8})$$

$$K_{5/3}(x) \rightarrow \sqrt{\frac{\pi}{2x}} e^{-x} \quad \text{for } x \rightarrow \infty \quad (\text{A.9})$$

Because α_ν is a monotonically decreasing function of x , we can define a unique $x_a(b, \gamma)$ where the optical depth $\tau_s = R\alpha_\nu$ for synchrotron absorption along a path of length R is unity:

$$R\alpha_\nu(x_a) = 1 \quad (\text{A.10})$$

If $x_a \ll 1$, we have *weak absorption* and for $x_a \gg 1$ *strong absorption*. The transition between the two regimes occurs near Lorentz factor γ_c , defined as

$$\gamma_c = \left(\frac{\tau_T}{2\sqrt{3}\alpha_f b \sin \theta} \right)^{1/5} \quad (\text{A.11})$$

so that

$$\begin{aligned} \tau_s &= \hat{\gamma}^{-5} K_{5/3}(x) \\ &= \frac{\sqrt{3}\tau_T mc^3 K_{5/3}(x)}{8\pi e^2 \nu_c \gamma^3} \end{aligned} \quad (\text{A.12})$$

where $\hat{\gamma} = \gamma/\gamma_c$. In the case of weak absorption,

$$x_a \approx 2^{2/5} [\Gamma(5/3)]^{3/5} / \hat{\gamma}^3 \quad \text{for } \hat{\gamma} \gg 1 \quad (\text{A.13})$$

whereas in the strong absorption regime

$$x_a \sim -5 \ln \hat{\gamma} \quad \text{for } \hat{\gamma} \ll 1 \quad (\text{A.14})$$

Taking account of synchrotron emission and absorption and ignoring the role of polarisation, the specific intensity in a direction which cuts the source on a path of length R is

$$I_\nu = S_\nu [1 - \exp(-\tau_s)] \quad (\text{A.15})$$

where the *source function* $S_\nu = j_\nu/\alpha_\nu$ is

$$S_\nu = \left(\frac{B^2}{8\pi} \right) \left(\frac{9e^2 \gamma_c^5}{2\pi mc^2} \right) \sin^2 \theta S(\hat{\gamma}, x) \quad (\text{A.16})$$

with

$$S(\hat{\gamma}, x) = \frac{\hat{\gamma}^5 F(x)}{K_{5/3}(x)} \quad (\text{A.17})$$

$$\rightarrow \begin{cases} \frac{2\pi}{\sqrt{3}\Gamma(1/3)\Gamma(5/3)} \hat{\gamma}^5 x^2 & \text{as } x \rightarrow 0 \\ \hat{\gamma}^5 x & \text{as } x \rightarrow \infty \end{cases} \quad (\text{A.18})$$

and the optical depth to synchrotron absorption τ_s is a function of $\hat{\gamma}$ and x .

To find the energy density U_s in synchrotron photons in a given source, I_ν must be integrated over angles and over frequency. The result depends on the geometry and optical depth as well as the position within the source. However, an average value can be estimated by introducing a geometry dependent factor $\zeta \approx 1$:

$$U_s \approx \frac{4\pi\zeta}{c} \int_0^\infty d\nu \langle I_\nu \rangle \quad (\text{A.19})$$

and denoting by $\langle I_\nu \rangle$ the specific intensity evaluated at $\theta = \pi/2$. Then

$$U_s = \zeta \left(\frac{B^2}{8\pi} \right) \left(\frac{27\alpha_f}{2\pi} \right) b \gamma_c^7 U(\hat{\gamma}) \quad (\text{A.20})$$

with

$$U(\hat{\gamma}) = \hat{\gamma}^2 \int_0^\infty dx S(\hat{\gamma}, x) \{1 - \exp[-\tau_s(\hat{\gamma}, x)]\} \quad (\text{A.21})$$

This integral is dominated by the region $x \gg x_a$ in the weak absorption regime:

$$\begin{aligned} U(\hat{\gamma}) &\approx \int_0^\infty dx S \tau_s \\ &= \int_0^\infty dx F(x) \\ &= \frac{8\pi\hat{\gamma}^2}{9\sqrt{3}} \quad \text{for } \hat{\gamma} \gg 1 \end{aligned} \quad (\text{A.22})$$

and by the region around $x = x_a$ in the strong absorption regime:

$$\begin{aligned} U(\hat{\gamma}) &\approx \int_0^{x_a} dx S \\ &\approx 12.5\hat{\gamma}^7 (\ln \hat{\gamma})^2 \quad \text{for } \hat{\gamma} \ll 1 \end{aligned} \quad (\text{A.23})$$

which suggests the simple approximation

$$U(\hat{\gamma}) \approx \frac{12.5\hat{\gamma}^7}{\left[0.183 + (\ln \hat{\gamma})^2\right]^{-1} + 7.75\hat{\gamma}^5} \quad (\text{A.24})$$

where the constant 0.183 was chosen such that the approximation passes through the point $U(1) = 0.945$ found by numerical integration.

References

- Begelman, M. C., Ergun, R. E., & Rees, M. J. 2005, *ApJ*, 625, 51
- Blundell, K., Fabian, A., Crawford, C., Erlund, M., & Celotti, A. 2006, *ArXiv Astrophysics e-prints*
- Cohen, M. H., Russo, M. A., Homan, D. C., et al. 2003, in *ASP Conf. Ser. 300: Radio Astronomy at the Fringe*, 177
- Crusius-Waetzel, A. R. 1991, *A&A*, 251, L5
- Fossati, G., Maraschi, L., Celotti, A., Comastri, A., & Ghisellini, G. 1998, *MNRAS*, 299, 433
- Gopal-Krishna, Biermann, P. L., & Wiita, P. J. 2004, *ApJ*, 603, L9

- Guainazzi, M., Siemiginowska, A., Stanghellini, C., et al. 2006, *A&A*, 446, 87
- Jones, T. W. & Burbidge, G. R. 1973, *ApJ*, 186, 791
- Jones, T. W. & Odell, S. L. 1977, *A&A*, 61, 291
- Kardashev, N. S. 2000, *Astronomy Reports*, 44, 719
- Kellermann, K. I. & Pauliny-Toth, I. I. K. 1969, *ApJ*, 155, L71
- Kirk, J. G. & Tsang, O. 2006, *A&A*, 447, L13
- Kraus, A., Krichbaum, T. P., Wegner, R., et al. 2003, *A&A*, 401, 161
- Lightman, A. P. & Zdziarski, A. A. 1987, *ApJ*, 319, 643
- Longair, M. S. 1992, *High energy astrophysics. Vol.1,2: Particles, photons and their detection* (Cambridge: Cambridge University Press, 1992, 2nd ed.)
- Macquart, J.-P. & de Bruyn, G. 2005, *ArXiv Astrophysics e-prints*
- Macquart, J.-P., Kedziora-Chudczer, L., Rayner, D. P., & Jauncey, D. L. 2000, *ApJ*, 538, 623
- Marscher, A. 1980, *Nature*, 288, 12
- Mastichiadis, A. & Kirk, J. G. 1995, *A&A*, 295, 613
- Ostorero, L., Wagner, S. J., Gracia, J., et al. 2006, *A&A*, 451, 797
- Padovani, P., Costamante, L., Giommi, P., et al. 2004, *MNRAS*, 347, 1282
- Protheroe, R. J. 2002, *Publications of the Astronomical Society of Australia*, 19, 486
- Protheroe, R. J. 2003, *MNRAS*, 341, 230
- Readhead, A. C. S. 1994, *ApJ*, 426, 51
- Rees, M. J. 1966, *Nature*, 211, 468
- Rees, M. J. 1967, *MNRAS*, 135, 345
- Rickett, B. J., Kedziora-Chudczer, L., & Jauncey, D. L. 2002, *ApJ*, 581, 103
- Rybicki, G. B. & Lightman, A. P. 1979, *Radiative processes in astrophysics* (New York, Wiley-Interscience, 1979. 393 p.)
- Sambruna, R. M., Chou, L. L., & Urry, C. M. 2000, *ApJ*, 533, 650
- Singal, K. A. & Gopal-Krishna. 1985, *MNRAS*, 215, 383
- Slysh, V. I. 1992, *ApJ*, 391, 453
- Tavecchio, F., Maraschi, L., Ghisellini, G., et al. 2002, *ApJ*, 575, 137
- Wagner, S. J. & Witzel, A. 1995, *ARA&A*, 33, 163
- Wardle, J. F. C. 1977, *Nature*, 269, 563